Development 134, 1767-1777 (2007) doi:10.1242/dev.02842

The F-actin–microtubule crosslinker Shot is a platform for Krasavietz-mediated translational regulation of midline axon repulsion

Seongsoo Lee[1,2], Minyeop Nahm[1], Mihye Lee[1,2], Minjae Kwon[3], Euijae Kim[1], Alireza Dehghani Zadeh[3], Hanwei Cao[3], Hyung-Jun Kim[2], Zang Hee Lee[1], Seog Bae Oh[4], Jeongbin Yim[2], Peter A. Kolodziej[3] and Seungbok Lee[1,*]

Axon extension and guidance require a coordinated assembly of F-actin and microtubules as well as regulated translation. The molecular basis of how the translation of mRNAs encoding guidance proteins could be closely tied to the pace of cytoskeletal assembly is poorly understood. Previous studies have shown that the F-actin–microtubule crosslinker Short stop (Shot) is required for motor and sensory axon extension in the *Drosophila* embryo. Here, we provide biochemical and genetic evidence that Shot functions with a novel translation inhibitor, Krasavietz (Kra, Exba), to steer longitudinally directed CNS axons away from the midline. Kra binds directly to the C-terminus of Shot, and this interaction is required for the activity of Shot to support midline axon repulsion. *shot* and *kra* mutations lead to weak *robo*-like phenotypes, and synergistically affect midline avoidance of CNS axons. We also show that *shot* and *kra* dominantly enhance the frequency of midline crossovers in embryos heterozygous for *slit* or robo, and that in *kra* mutant embryos, some Robo-positive axons ectopically cross the midline that normally expresses the repellent Slit. Finally, we demonstrate that Kra also interacts with the translation initiation factor eIF2β and inhibits translation in vitro. Together, these data suggest that Kra-mediated translational regulation plays important roles in midline axon repulsion and that Shot functions as a direct physical link between translational regulation and cytoskeleton reorganization.

KEY WORDS: *kra*, *shot*, Translation, Axon guidance, CNS, *Drosophila*

INTRODUCTION

The developmentally stereotyped migrations of neuronal growth cones establish an initial network of neuronal connections that is crucial for proper nervous system function. Chemical gradients or local cues presented on cellular landmarks guide these migrations by controlling dynamic rearrangements of the growth cone cytoskeleton (Dent and Gertler, 2003; Dickson, 2002). As growth cones encounter these cues, they adapt their responses. When reading a chemical gradient, growth cones continuously reset their threshold sensitivity to the cue so that higher concentrations elicit cytoskeletal responses required for motility and guidance (Song and Poo, 2001). Locally presented cues may also qualitatively change growth cone responsiveness, enabling them to proceed to the next cellular target in the pathway (Song and Poo, 2001).

Growth cone adaptation may require new local protein synthesis (Dickson, 2002). Axonal or dendritic transport may not be fast enough to supply proteins to growth cones at a distance from the cell body. Axotomy experiments with protein synthesis inhibitors indicate that new protein synthesis in axons or their growth cones is required for turning in vitro in response to extracellular gradients of guidance cues (Campbell and Holt, 2001; Ming et al., 2002). Local protein synthesis is also required for growth cones to change their responsiveness to specific local cues. In the spinal cord of vertebrates, translation of *ephA2* receptor mRNA is locally regulated, occurring in commissural growth cones only after they cross the midline (Brittis et al., 2002). Translational regulation in axons and their growth cones may involve rapamycin- or MAP kinase (MAPK)-sensitive pathways (Campbell and Holt, 2001; Campbell and Holt, 2003; Ming et al., 2002), and also cytoplasmic polyadenylation element (CPE)-dependent mechanisms (Brittis et al., 2002). However, the mechanism connecting receptor signaling to translation is largely unknown.

In the *Drosophila* embryo, the midline repellent Slit prevents longitudinally directed CNS axons from crossing the midline (Kidd et al., 1999) and directs them into particular longitudinal pathways through its Robo, Robo2 and Robo3 receptors on the CNS growth cones (Kidd et al., 1999; Simpson et al., 2000). As we show here, the spectraplakin Short stop (Shot; also known as Kakapo) is also required for midline axon repulsion. Mutations in *shot* lead to ectopic midline crossing of Fas II-positive axons and dominantly enhance the *slit* or *robo* heterozygous loss-of-function phenotypes, suggesting that *shot* may function in the same guidance process as *slit* and *robo*.

Shot mediates direct interactions between F-actin and microtubules (MTs) required for initial sensory axon extension and motor axon extension to target muscles (Lee and Kolodziej, 2002b). We provide evidence that the role of Shot in midline guidance involves translational regulation. Shot physically interacts with Krasavietz (Kra; also known as Exba), an evolutionarily conserved putative translation factor, and this interaction is required for Shot activity to support midline axon repulsion. Kra contains a C-terminal W2 domain found in the translation initiation factors eIF5, eIF2Bϵ, DAP-5 and eIF4G. The W2 domains in these translation initiation factors have been shown to mediate protein-protein interactions among translation factors that are required for preinitiation complex assembly (Preiss and Hentze, 2003). As suggested by the presence of W2 domain, Kra binds to eIF2β and 40S ribosomal subunits. We

[1]Department of Cell and Developmental Biology, School of Dentistry, Seoul National University, Seoul 110-740, Republic of Korea. [2]School of Biological Sciences, College of Natural Sciences, Seoul National University, Seoul 151-742, Republic of Korea. [3]Department of Cell and Developmental Biology, Vanderbilt University Medical Center, Nashville, TN 37232-2175, USA. [4]Department of Physiology, School of Dentistry, Seoul National University, Seoul 110-740, Republic of Korea.

*Author for correspondence (e-mail: seunglee@snu.ac.kr)

Accepted 22 February 2007

also show that Kra inhibits translation in vitro. Finally, we show that in *kra* or *eIF2β* mutant embryos some Robo-expressing axons lose the ability to respond to the midline repellent Slit. Taken together, our data suggest that Shot functions as a platform for translational control of midline axon guidance. Through this proposed Shot-Kra-eIF2β circuit, the translation of mRNAs encoding proteins essential for axon guidance at the midline may be closely tied to the pace of cytoskeletal assembly.

MATERIALS AND METHODS

Molecular biology

All full-length cDNA clones for *kra*, *eIF5* and *eIF2β* were obtained from the *Drosophila* Genomics Resource Center (GenBank accession numbers AA440023, AW941924 and BI23305, respectively). For glutathione S-transferase (GST) pull-down assays, the full-length coding sequences of *kra* and *eIF5* were amplified by polymerase chain reaction (PCR) and subcloned into pGEX6P1 (Pharmacia). For in vitro translation, the full-length coding regions of *eIF2β* were subcloned into pCDNA3.1 (Invitrogen). The C-terminal domain of the Shot long isoforms, C-Shot L [amino acids (AA) 4689 to 5201; GenBank accession number AAF24343], and its deletions were amplified by PCR and subcloned into pSP64 Poly(A) (Promega). For the *kra* rescue experiments, the coding sequence of *kra* was tagged with hemagglutinin (HA) and subcloned into pUASTNEXT (Lee and Kolodziej, 2002a), a derivative of the pUAST vector (Brand and Perrimon, 1993), to give *UAS-HA-kra^{WT}*. The wild-type *kra* cDNA was manipulated using the QuikChange Multi kit (Stratagene) to introduce the 12A and 7A mutations (Fig. 1B). The insert of *UAS-HA-kra^{WT}* was replaced with *kra^{12A}* and *kra^{7A}* cDNAs to give *UAS-HA-kra^{12A}* and *UAS-HA-kra^{7A}*, respectively. To overexpress *eIF2β* in the fly embryo, the entire coding sequence was tagged with green fluorescent protein (GFP) and introduced into pUASTNEXT.

Genetics

Two P-element insertions in the *kra* locus, *l(3)j9b6* (Bloomington Stock Center, Bloomington, IN) and *EP(3)0428* (Szeged Stock Center, Hungary), were obtained and mobilized by standard methods to generate *kra^{1}* and *kra^{2}*, respectively. For the *kra* rescue experiments, transgenic flies expressing *UAS-HA-kra^{WT}*, *UAS-HA-kra^{7A}* and *UAS-HA-kra^{12A}* cDNAs were obtained as previously described (Robertson et al., 1988). These transgenes were expressed in the *kra^{1}/kra^{2}* mutant embryos under the control of *da-GAL4* (Wodarz et al., 1995), *C155-GAL4* (Lin and Goodman, 1994), *repo-GAL4* (Sepp et al., 2001) or *slit-GAL4* (Scholz et al., 1997). *shot* rescue experiments were performed as previously described (Lee and Kolodziej, 2002b). *slit^{2}* and *robo^{2}* were obtained from the Bloomington *Drosophila* Stock Center.

Cell culture and double-stranded RNA interference

S2 cells were grown at 29°C in Schneider's medium (Invitrogen) supplemented with 10% heat-inactivated (30 minutes, 55°C) fetal calf serum. S2 cells were transfected using Cellfectin (Invitrogen) according to the manufacturer's instructions.

Double-stranded RNA interference (dsRNAi) was performed in six-well tissue culture plates containing 2×10^{6} S2 cells for 3 days as previously described (Clemens et al., 2000). Briefly, DNA templates containing T7 promoter sequences at their 5′ and 3′ ends were amplified by PCR and transcribed with the Megascript T7 transcription kit (Ambion) to generate dsRNAs. Primers contained T7 promoter sequences upstream of the following: *kra* sense primer, 5′-TTGGTCCACCATCATGTCATT-3′, *kra* antisense primer, 5′-ACTGAAGCCATTCGACAAAC-3′; *gfp* sense primer, 5′-ACGTAAACGGCCACAAGTTC-3′, *gfp* antisense primer, 5′-GTCC-TCCTTGAAGTCGATGC-3′. For the assay, dsRNAs were used at a final concentration of 37 nM.

Antibodies and immunohistochemistry

In order to raise antibodies against the full-length Kra and eIF2β proteins, GST-Kra and MBP-eIF2β were expressed in *Escherichia coli* BL21 (Stratagene) and purified with glutathione-Sepharose 4B (Amersham Pharmacia) and amylose resin (NEB), respectively. GST-Kra was digested with PreScission protease (Amersham Pharmacia). Protein samples were subjected to SDS-polyacrylamide gel electrophoresis (SDS-PAGE), and the bands representing 50 kDa Kra and 82 kDa MBP-eIF2β were excised for the immunization of guinea pigs and rats, respectively.

Monoclonal antibodies (mAbs) against Fasciclin II (1D4), Repo (8D12), Wrapper (10D3), Robo (13C9) and Slit (C555.6D) were purchased from the Developmental Studies Hybridoma Bank (DSHB). Additional antibodies used in this study were rabbit anti-eIF4E (Nakamura et al., 2004), 3F10 rat monoclonal anti-HA (Roche), rabbit anti-β-galactosidase (Cappel), rabbit anti-GFP (Abcam), rabbit anti-horseradish peroxidase (HRP) (MP Biochemicals) and goat anti-L28 (Santa Cruz).

Whole-mount staining of embryos was performed as previously described (Lee et al., 2000; Spencer et al., 1998).

Binding experiments

For GST pull-down assays, GST fusion proteins of Kra and eIF5 were produced in *E. coli* and purified using glutathione-Sepharose 4B (Amersham Pharmacia). eIF2β and the C-terminal regions of the Shot long isoforms were synthesized using an in vitro transcription/translation kit (Promega) in the presence of [^{35}S]methionine. The binding of GST-Kra to the C-terminal regions of Shot was performed in 20 mM Tris-HCl (pH 7.5), 1 mM $CaCl_2$, 1% NP-40, 150 mM NaCl, 5 mM DTT and 10% glycerol, or in 20 mM Tris-HCl (pH 7.5), 1 mM EGTA, 0.1% NP-40, 150 mM NaCl, 5 mM DTT and 10% glycerol. The additional binding experiment was performed in a binding buffer containing 20 mM Tris-HCl (pH 8.0), 200 mM NaCl, 1 mM EDTA and 0.5% NP-40.

For immunoprecipitation, fly embryos or S2 cells coexpressing HA-Kra with GFP-eIF2β, Shot L(A)-GFP or C-Shot L-GFP were homogenized in immunoprecipitation buffer [50 mM Tris-HCl (pH 8.0), 1% NP-40, 150 mM NaCl, 2 mM Na_3VO_4, 10 mM NaF, 10% glycerol, protease inhibitors], and then centrifuged at 12,000 ***g*** for 25 minutes at 4°C. Supernatants were precleared by incubation with protein G-Sepharose (Pierce) for 1 hour at 4°C. The samples were incubated with anti-GFP or anti-HA for 4 hours at 4°C and then incubated with protein G-Sepharose for 2 hours at 4°C. Beads were washed three times with immunoprecipitation buffer and boiled in SDS sample buffer. The eluates were subjected to western blotting.

In vitro translation assays

For in vitro translation, rabbit reticulocyte lysate (Promega) was first preincubated with 2.4 μM bovine serum albumin (BSA), GST, GST-Kra, Kra or Kra-7A. Each translation reaction contained 50% rabbit reticulocyte lysate, 1×TNT reaction buffer (Promega), 40 μM AA mixture without methionine (Promega), 10 μCi [^{35}S]methionine (Amersham Pharmacia), 20 U of RNase inhibitor (Promega) and 70 nM *luciferase* mRNA. After incubating the reaction for 90 minutes at 30°C, 20% of each reaction was removed and analyzed by SDS-PAGE and autoradiography to monitor the translation output.

Sucrose gradient analysis

S2 cell extracts were prepared in lysis buffer [50 mM Tris-HCl (pH 7.5), 250 mM NaCl, 50 mM $MgCl_2$, 100 μg/ml heparin, 1 mM DTT and 0.5 mg/ml cycloheximide]. Cell lysates were layered on 7-47% (w/v) linear sucrose gradients in the lysis buffer, and centrifuged at 270,000 ***g*** for 3 hours at 4°C in a Beckman SW41 rotor. Fractions were collected from the top of the gradient and analyzed for absorbance at 260 nm to locate the ribosomal subunits (40S, 60S and 80S) and polysomes. Portions of fractions were further analyzed by SDS-PAGE and western blotting.

RESULTS

Shot associates with the putative translation factor Kra

Through alternative splicing and multiple promoter usage, *shot* encodes multiple, modularly assembled protein isoforms. Neuronal expression of either the Shot L(A) or Shot L(B) isoform in *shot* mutant embryos rescues defects in sensory and motor axon extension to target muscles (Lee and Kolodziej, 2002b). These isoforms contain both an N-terminal F-actin binding domain (ABD)

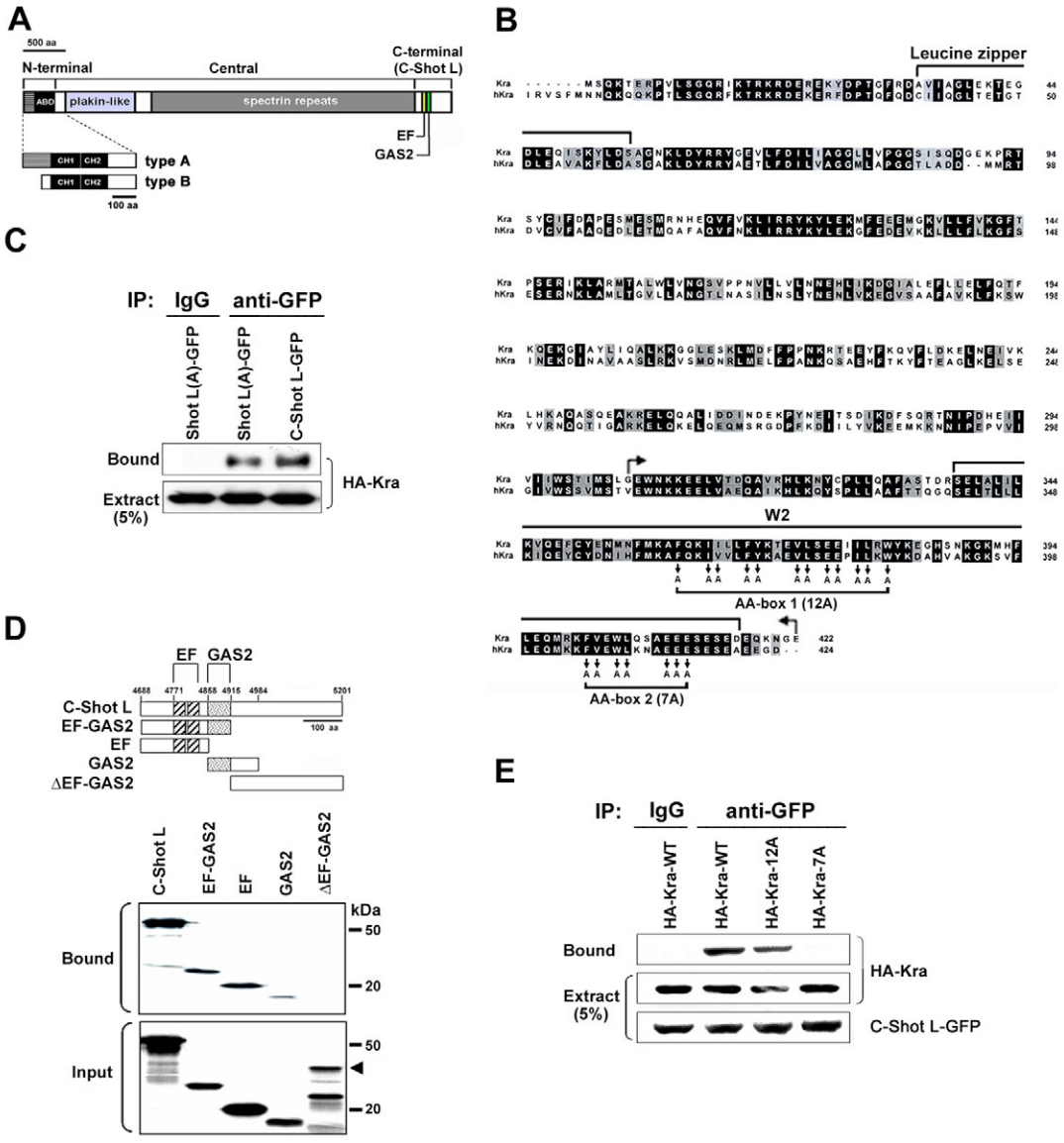

Fig. 1. Shot is physically associated with the translation initiation factor Kra/eIF5C. (**A**) Domain structure of the evolutionarily conserved Shot isoforms, Shot L(A) and Shot L(B). ABD, actin-binding domain; CH, calponin homology motif; EF, EF-hand motif; GAS2, GAS2 homology motif. (**B**) Sequence comparison of Kra with human Kra/BZAP45 (GenBank accession number BAA02795). Sequence identities (51%) are indicated by white letters on a black background, and sequence similarities (+1 or more in a PAM 250 matrix) are indicated by black letters on a gray background. N-terminal leucine zipper and C-terminal W2 domains are indicated above the sequences. Multiple alanine substitutions 12A and 7A, which were introduced into the AA-boxes 1 and 2, respectively, are also shown within the W2 domain. The boundaries of the *kra* cDNAs isolated from the yeast two-hybrid screen are marked by bent arrows. (**C**) Shot physically interacts with Kra. Soluble extracts of S2 cells transiently expressing HA-tagged Kra with Shot L(A)-GFP or C-Shot L-GFP were immunoprecipitated with IgG or anti-GFP antibody. The precipitates were subjected to SDS-PAGE and western blot analysis using anti-HA. (**D**) A region covering the EF-hand motifs of Shot is largely responsible for its interaction with Kra. In pull-down assays, GST-Kra was incubated with [^{35}S]methionine-labeled C-terminal fragments of Shot containing AA residues 4688-5201 (C-Shot L), 4688-4915 (EF-GAS2), 4688-4858 (EF), 4859-4984 (GAS2) and 4916-5201 (ΔEF-GAS2, an arrowhead). The relative input of the labeled proteins (20% of the amount used in each reaction) is shown in the bottom panel. (**E**) The AA-box 2 in Kra is essential for its interaction with Shot. Soluble extracts from S2 cells expressing C-Shot L-GFP with HA-Kra^{WT}, HA-Kra^{12A} or HA-Kra^{7A} were immunoprecipitated with IgG or anti-GFP. The presence of HA-Kra in the precipitates was detected by western blot analysis using anti-HA.

and a C-terminal domain (C-Shot L) with two putative Ca^{2+}-binding (EF-hand) and microtubule-binding (GAS2) motifs (Fig. 1A), all of which are essential for axon extension (Lee and Kolodziej, 2002b). To investigate the function of the C-terminal motifs, we performed a yeast two-hybrid screen with a *Drosophila* embryonic cDNA library using C-Shot L (AAF24343, residues 4688 to 5201) as a bait. Two of the interacting clones encoded the C-terminal domain (residues 315 to 422) of a novel protein, Krasavietz (Kra), which has been annotated in FlyBase as CG2922. The predicted Kra protein is 51-52% identical to its *Xenopus* (AAH41729), zebrafish (AAH58875), mouse (AAH05466) and human (hKra/BZAP45; BAA02795) homologs (Fig. 1B and data not shown). However, no Kra homologs have been identified in yeast or *Caenorhabditis elegans*.

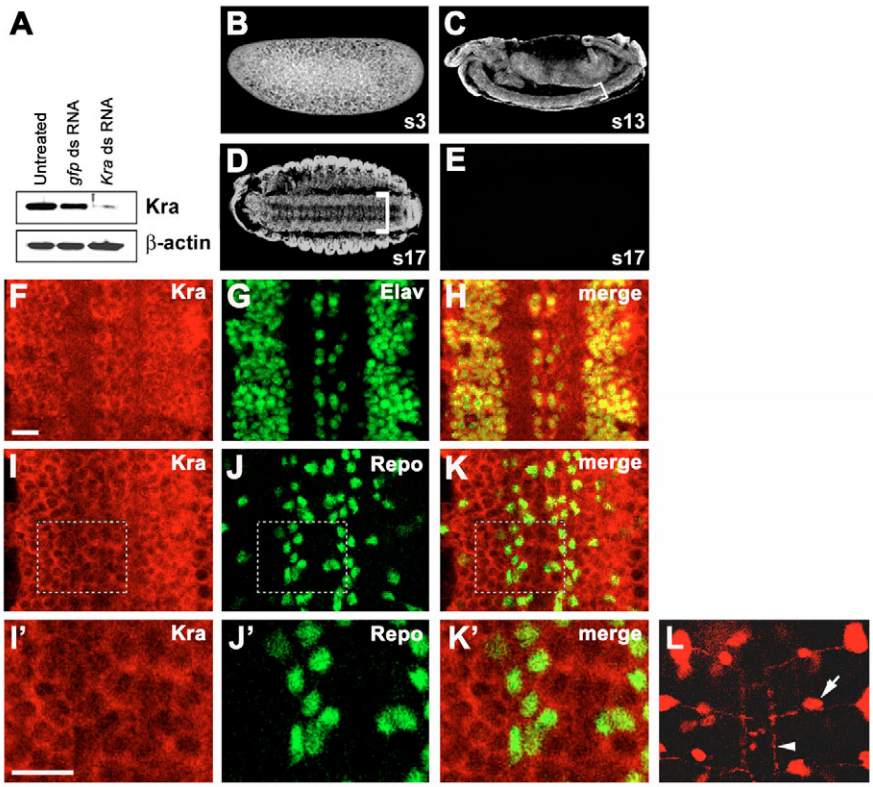

Fig. 2. Kra is expressed in the embryonic CNS. (**A**) Western blot analysis of S2 cell extracts using anti-Kra. The recognized protein is significantly depleted in *kra* RNAi-treated cells but not in *gfp* RNAi-treated control cells. (**B-D**) Whole-mount wild-type embryos stained with anti-Kra. Brackets mark the ventral nerve cord (VNC). (B) A stage 3 embryo. Lateral view. (C) A stage 13 embryo. Lateral view. (D) A stage 16 embryo. Ventral view. (**E**) A stage 16 embryo stained with preimmune serum. Ventral view. (**F-H**) A confocal section (1 μm) of a stage 16 wild-type embryo labeled with anti-Kra (F) and anti-Elav (G). (H) Merge of F and G. (**I-K**) A confocal section (1 μm) of a stage 16 wild-type embryo labeled with anti-Kra (I) and anti-Repo (J). (K) Merge of I and J. (**I′-K′**) Higher magnification of the area marked with white broken lines in I-K. (**L**) The CNS of embryos, carrying both *ap-GAL4* and *UAS-HA-Kra*^{WT}, stained with anti-HA. HA-Kra protein is detected in both the bodies (arrow) and the axons (arrowhead) of the Ap neurons. Scale bars: in F, 10 μm for F-L; in I′, 10 μm for I′-K′.

To confirm Shot-Kra interaction, we coexpressed either Shot L(A)-GFP or C-Shot L-GFP with HA-Kra in S2 cells and performed coimmunoprecipitation experiments. We found that Shot L(A)-GFP specifically coimmunoprecipitated with HA-Kra (Fig. 1C). C-Shot L-GFP also formed complexes with HA-Kra with affinities comparable to that of Shot L(A)-GFP (Fig. 1C), suggesting that the C-terminal domain of Shot is largely responsible for its interaction with Kra.

Next, we performed GST pull-down assays to determine the Kra-binding motif in C-Shot L. GST-Kra efficiently bound to fragments of C-Shot L containing either the EF-hand and GAS2 motifs (EF-GAS2) or the EF-hand motifs only (EF), whereas the GAS2-containing fragment by itself showed Kra binding activity at lower levels (Fig. 1D). By contrast, ΔEF-GAS2, which removes both the EF-hand and the GAS2 motifs from C-Shot L, did not bind to GST-Kra (Fig. 1D). The importance of the EF-hand and GAS2 motifs for Shot-Kra interaction was further evaluated in S2 cells. We found that binding of Shot L(A)-GFP to HA-Kra was reduced to 5% by deletion of the EF-hand motifs and to 35% by deletion of the GAS2 motif (see Fig. S1 in the supplementary material). These observations indicate that the EF-hand motifs are the major Kra-binding sites, and that the GAS2 motif is also required for strong interactions. Interestingly, Shot L(A)-ΔEF-GFP bound endogenous α-tubulin at comparable levels to Shot L(A)-GFP (see Fig. S1 in the supplementary material), suggesting that Kra binding through the EF-hand motifs does not impair the ability of Shot to bind microtubules through the GAS2 motif.

The two-hybrid screen result indicates that the C-terminal domain of Kra contains the Shot binding site. A database search revealed that the region belongs to the W2 domain family found in translation initiation factors. Multiple alanine substitutions (12A and 7A in the AA-boxes 1 and 2, respectively) in the W2 domain of eIF5 disrupt its interactions with eIF2β and eIF3-NIP1 (Asano et al., 1999). To pinpoint the Shot binding site with regard to possible translation initiation factor binding sites, we made similar alanine substitutions in Kra (Fig. 1B). The Kra-12A mutant, as well as the wild-type Kra, efficiently bound C-Shot L in S2 cells, whereas the binding of C-Shot L with the Kra-7A mutant was minimal, appearing only at background levels (Fig. 1E). These data suggest that the evolutionarily conserved residues in the AA-box 2 motif of Kra are essential for Shot-Kra interaction.

Kra protein strongly accumulates in the embryonic CNS

We developed an antibody against full-length Kra, which detects a single 50-kDa band on western blots containing extracts of S2 cells (Fig. 2A). Levels of the recognized protein were significantly reduced by *kra* dsRNAi, but not by *gfp* dsRNAi, suggesting the specificity of our anti-Kra antibody (Fig. 2A). Immunostaining using anti-Kra revealed that Kra was highly expressed in early stage embryos (e.g. stage 3; Fig. 2B) because of a significant maternal contribution. It was detected in the CNS and epidermis by stage 11, and in the gut by stage 13 (Fig. 2C). High expression in the CNS was maintained until the end of embryogenesis (Fig. 2D).

We inspected the embryonic CNS by double labeling with anti-Kra and anti-Elav, a neuronal marker (Lin and Goodman, 1994), and found that Kra is expressed in most or all post-mitotic neurons (Fig. 2F-H). Kra localized primarily to the cytoplasm of those cells, but was not clearly detectable in CNS axons (Fig. 2H). Kra was also expressed in many CNS glial cells (Fig. 2I-K), as assessed by double labeling with anti-Kra and anti-Repo, a glial marker that visualizes CNS glial cells, except for the midline glia (Halter et al., 1995). To assess the expression of Kra in midline glial cells, we used a midline glial marker anti-Wrapper (Noordermeer et al., 1998). However, because of ubiquitous expression of Kra around the midline, we were not able to determine its presence in these cells. We next

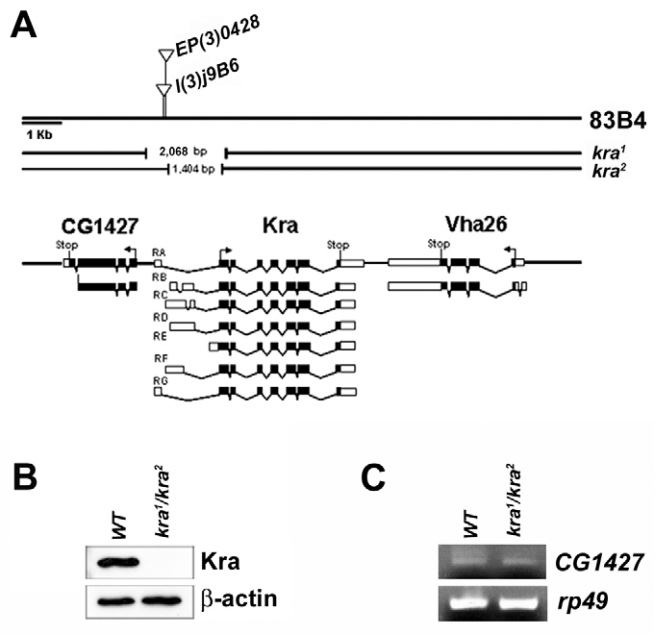

Fig. 3. *kra*-null mutants. (**A**) Genomic organization of the *kra* locus. *CG1427* and *Vha26* genes are flanking the *kra* locus at position 83B4 on the right arm of the third chromosome. The relative positions of P-element insertions *l(3)j9B6* and *EP(3)0428* are indicated as inverted triangles. The extents of deletions in kra^1 and kra^2 are indicated. For the predicted transcripts, black boxes represent coding regions and white boxes represent untranslated regions; predicted translation initiation and stop sites are indicated. (**B**) Western blot analysis of larval extracts using anti-Kra. The same blot was reprocessed with anti-β-actin to confirm equal protein loading. (**C**) RT-PCR analysis of *CG1427* and *rp49* expression in third instar wild-type and kra^1/kra^2 mutant larvae.

wished to examine the localization of Kra at single axon resolution. We therefore expressed *UAS-HA-Kra*^{WT} in a small subset of embryonic CNS neurons with the aid of a neuronal driver *apterous* (*ap*)-*GAL4* (O'Keefe et al., 1998). HA-Kra was strongly detected in the cell body and the axon of the Ap neurons (Fig. 2L), suggesting that Kra can be localized into axons.

Generation of *kra*-null mutants

Partial loss-of-function P-element alleles of *kra* affect learning and memory (Dubnau et al., 2003). To determine its role in neuronal development, we generated molecularly defined *kra*-null mutants. We first verified that the transposons of *l(3)j9B6* and *EP(3)0428* were inserted at –1636 and –1228, respectively, of the *kra* open reading frame (ORF), which is common to its multiple transcript variants (Fig. 3A). We then mobilized these P-elements, recovered 200 independent excision lines from each parental allele, and determined the breakpoints of 30 lethal alleles by PCR and DNA sequencing. In particular, we found that kra^1, derived from *l(3)j9B6*, deletes 2068 bp (–1729 to +338), whereas kra^2, derived from *EP(3)0428*, deletes 1404 bp (–1242 to +161). Both deletions remove most of the 5′-UTR and the translation start site, and extend into the ORF (Fig. 3A). Homozygotes and transheterozygotes for these deletion alleles died at the pupal stage. The anti-Kra antibody cleanly detected the Kra protein in wild-type, but not in kra^1/kra^2 mutant larvae or pupae (Fig. 3B and data not shown), suggesting that both kra^1 and kra^2 are null alleles for *kra*.

The *kra* gene is located 463 bp upstream of the putative gene *CG1427*, whose function is unknown. Reverse transcription (RT)-PCR analysis showed that levels of *CG1427* mRNA were normal in kra^1/kra^2 third instar larvae (Fig. 3C), suggesting that kra^1 and kra^2 mutations do not affect the expression of *CG1427*.

kra is required in neurons for CNS axon pathfinding

We next investigated whether axon extension and guidance are defective in *kra*-null mutant embryos. No defects in sensory and motor extension were observed in kra^1/kra^2 embryos stained with mAb 22C10 or 1D4 (data not shown). We then examined axon phenotypes in the CNS. In wild-type embryos at early stage 13, mAb 1D4 labeled the pCC axon that pioneers the ipsilateral pCC pathway without crossing the midline (Fig. 4A). In kra^1/kra^2 embryos, the same axon aberrantly often crossed the midline (Fig. 4B). This early-stage axon pathway defect indicates that *kra* is required for accurate growth cone migration. This phenotype becomes more obvious in later stage embryos. In wild-type embryos at stage 16, mAb 1D4 labeled three longitudinal axon pathways on each side of the midline; axons in these pathways did not cross the midline (Fig. 4D). In kra^1/kra^2 embryos, axons from the innermost (pCC) pathway ectopically crossed the midline in 18% of CNS segments (Fig. 4E,L). Kra is ubiquitously expressed in glial cells and neurons of the embryonic CNS. To determine where Kra functions in midline axon guidance, we examined CNS axon development in kra^1/kra^2 embryos that express *UAS-HA-kra*^{WT} under a neuron-specific driver *C155-GAL4*. In these embryos, only 6% of CNS segments exhibited the midline crossing defect (Fig. 4F,L), suggesting that Kra functions, at least in part, in neurons to enable growth cones to avoid the midline. By contrast, glial-specific expression of *UAS-HA-kra*^{WT} using *slit-GAL4* or *repo-GAL4* did not improve the *kra* midline phenotype (19% with *slit-GAL4*, n=464; 18% with *Repo-GAL4*, n=512).

kra-null mutant embryos contain substantial amounts of maternally contributed Kra protein. To generate embryos that lack maternally and zygotically contributed Kra, we used the FRT/ovoD1 method (Chou et al., 1993) to generate females containing homozygous kra^1 germline clones. These females did not lay eggs, and dissected germlines were blocked in oogenesis (data not shown). Kra therefore appears to be required during oogenesis, precluding isolation of embryos lacking maternally and zygotically contributed Kra.

kra and *shot* together control midline axon repulsion

In $shot^3$ mutant embryos, motor axons extend outward from the CNS, choosing the right pathways but then stalling short of their muscle targets (Lee et al., 2000). Sensory axons also extend appropriately during early parts of their trajectory but fail to advance (Lee et al., 2000). CNS axon phenotypes for *shot* have not been previously described. In the present study, we found that Fas II-positive CNS axons ectopically cross the midline in ~16% of segments in $shot^3$ embryos (Fig. 4C,G), suggesting the role of Shot in midline axon guidance. Neuronal expression of Shot L(A)-GFP rescued the midline crossing phenotype of $shot^3$ embryos (Fig. 4L). We have shown previously that the F-actin–microtubule crosslinking activity of Shot is essential for axon extension (Lee and Kolodziej, 2002b), and therefore we investigated whether this would still be the case for midline axon guidance. The microtubule-binding domain mutant Shot L(A)-ΔGAS2-GFP rescued the CNS phenotype of $shot^3$ embryos (Fig. 4H,L),

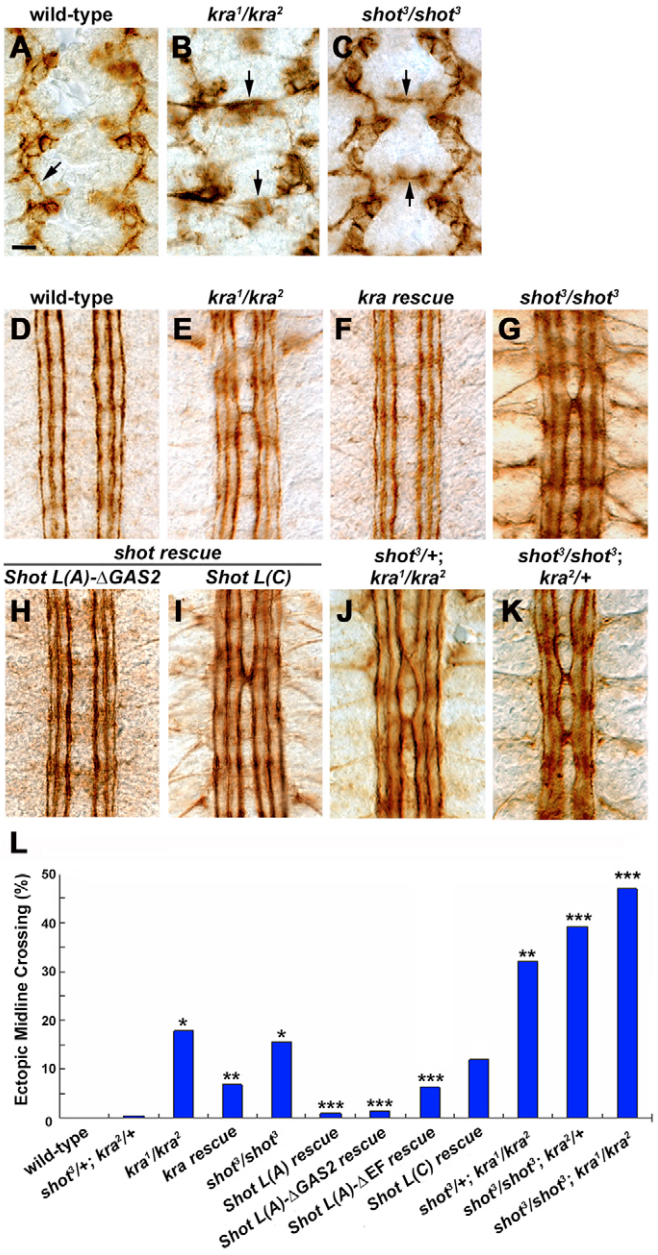

Fig. 4. *kra* and *shot* synergistically interact to affect CNS midline repulsion. (**A-K**) The CNS of embryos stained with mAb 1D4 (anti-Fasciclin II). (A-C) Early stage 13 embryos. (D-K) Stage 16-17 embryos. (A-I) Both *kra* and *shot* are required for midline axon repulsion. (A) In wild-type embryos, the pCC axon extends anteriorly and slightly away from the midline (arrow). (B,C) In kra^1/kra^2 (B) and $shot^3/shot^3$ (C) mutant embryos, the pCC axon abnormally crosses the midline (arrows). (D) The Fas II-positive axons show three parallel longitudinal pathways on each side of the midline in wild-type embryos. (E,G) The innermost pathway ectopically crosses the midline in kra^1/kra^2 (E) and $shot^3/shot^3$ (G) mutants. (F) The kra^1/kra^2 mutant phenotype is rescued by expressing the *UAS-HA-Kra*^{WT} transgene in all neurons. (H,I) The indicated transgenes are expressed in all neurons in $shot^3$ as described (Lee and Kolodziej, 2002b). (H) The midline phenotype of *shot* is rescued by the *UAS-Shot L(A)-ΔGAS2-GFP* transgene. (I) The *UAS-Shot L(C)-GFP* transgene fails to rescue the midline phenotype of *shot*. (J,K) Heterozygosity for *kra* and *shot* enhances the phenotypes of the *shot* and *kra* homozygotes, respectively, resulting in multiple crossing defects in $shot^3/+$; kra^1/kra^2 (J) and $shot^3/shot^3$; $kra^2/+$ (K) embryos. Anterior is to the top. (**L**) Quantification of midline crossing defects per segments in each of the indicated genotypes (wild-type, n=60 segments; $shot^3/+$; $kra^2/+$, n=240; kra^1/kra^2, n=504; *C155-GAL4/+*; kra^1,*UAS-HA-kra*^{WT}$/kra^2$, n=440; $shot^3/shot^3$, n=272; $shot^3$,*1407-GAL4/shot*^{3}; *UAS-Shot L(A)-GFP/+*, n=192; $shot^3$,*1407-GAL4/shot*^{3},*UAS-Shot L(A)-ΔGAS2-GFP*, n=264; $shot^3$,*1407-GAL4/shot*^{3},*UAS-Shot L(A)-ΔEF-GFP*, n=640; $shot^3$,*1407-GAL4/shot*^{3},*UAS-Shot L(C)-GFP*, n=816; $shot^3/+$; kra^1/kra^2, n=184; $shot^3/shot^3$; $kra^2/+$, n=120; $shot^3/shot^3$; kra^1/kra^2, n=298). Statistically significant differences, as determined by Student's t-test, are denoted by an asterisk (control, wild-type; P<0.001), double asterisk (control, kra^1/kra^2; P<0.017) or triple asterisk (control, $shot^3/shot^3$; P<0.001). Scale bar: 10 μm.

although the same transgene did not rescue their axon extension phenotypes as was previously described (Lee and Kolodziej, 2002b). By contrast, the F-actin-binding mutant Shot L(C)-GFP (Lee and Kolodziej, 2002b) was unable to rescue the loss of *shot* function in the embryonic CNS (Fig. 4I,L). These results suggest that midline axon repulsion requires the F-actin-binding activity of Shot, but neither the microtubule binding nor the F-actin–microtubule crosslinking activity. Shot L(A)-ΔEF-GFP showed only partial activity to improve the midline crossing defect in $shot^3$ mutant embryos (Fig. 4L), suggesting that Kra binding through the EF-hand motifs is also important for the role of Shot in midline axon repulsion.

To determine the physiological relevance of the biochemical interaction of Kra with Shot and phenotypic overlap between *kra* and *shot* at the midline, we investigated genetic interactions between *kra* and *shot*. The frequency of midline crossovers was significantly worse in $shot^3/+$; kra^1/kra^2 and $shot^3/shot^3$; $kra^2/+$ mutant embryos than in either homozygous kra^1/kra^2 or $shot^3/shot^3$ mutant embryos (Fig. 4J-L). The midline crossing phenotype in $shot^3/shot^3$; kra^1/kra^2 double mutant embryos was slightly worse than that in $shot^3/shot^3$; $kra^2/+$ mutant embryos (Fig. 4L). In a control experiment, $shot^3/+$; $kra^2/+$ embryos showed no significant midline defects (Fig. 4L). These dosage-sensitive genetic interactions, coupled with their biochemical interactions, suggest that Kra and Shot function together to control midline axon repulsion.

kra and *shot* interact with the midline repellent pathway

The phenotype observed in *kra* and *shot* mutants is qualitatively identical to that seen in *robo* mutants (Kidd et al., 1998), suggesting a link between Kra/Shot and the Slit/Robo repellent pathway. To test this hypothesis, we examined transheterozygous interactions of *kra* and *shot* with *robo*. In a control experiment, neither $kra^2/+$ nor $shot^3/+$ embryos showed significant axonal defects at the midline (Fig. 5A,B). In embryos heterozygous for $robo^2$, we rarely observed ectopic midline crossing of Fas II-positive axons (Fig. 5C). However, the phenotype was dramatically enhanced in transheterozygous $robo^2/+$; $kra^2/+$ or $shot^3$,$robo^2/+$ embryos (>17-fold; Fig. 5D,E,G). The phenotype was further increased in embryos transheterozygous for *shot*, *kra* and *robo* (Fig. 5F,G). Similar genetic interactions were also observed between *kra*, *shot* and *slit* (see Fig. S2 in the supplementary material). Thus, *kra* and *shot* genetically interact with *robo* and *slit*, suggesting that all these genes may function in the same guidance process.

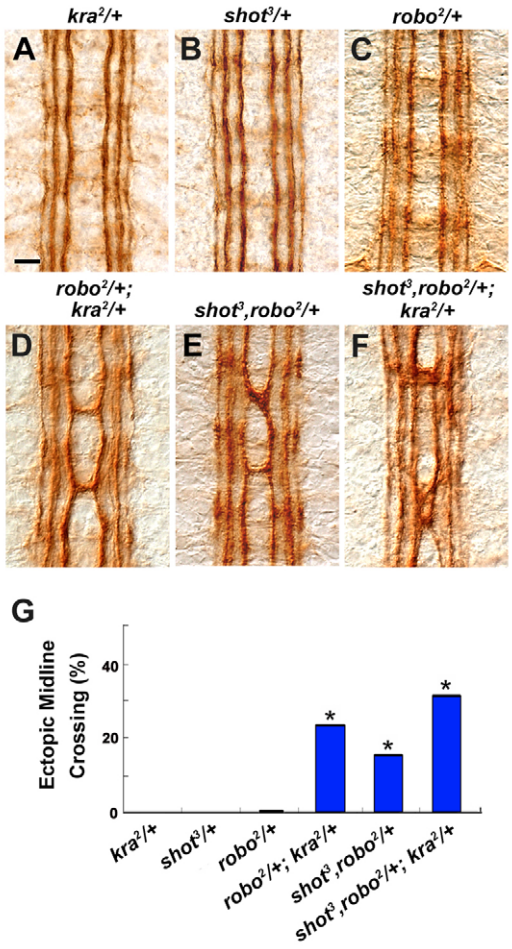

Fig. 5. *kra* and *shot* genetically interact with *robo*. (**A-F**) The CNS in stage 16-17 embryos stained with mAb 1D4 (anti-Fasciclin II). In *kra*^{2}/+ (A) or *shot*^{3}/+ (B) heterozygous embryos, the longitudinal axon tracts never cross the midline as in the wild-type (see Fig. 4D). (C) In *robo*^{2}/+ heterozygous embryos, the longitudinal axon tracts rarely cross the midline (0.9%). (D,E) The *robo*^{2}/+ phenotype is significantly enhanced when one copy of *kra* and *shot* is also removed in *robo*^{2}/+; *kra*^{2}/+ (D) or *shot*^{3},*robo*^{2}/+ (E) transheterozygous embryos. (F) This phenotype is also further enhanced in *shot*^{3},*robo*^{2}/+; *kra*^{2}/+ embryos. Anterior is to the top. (**G**) Quantification of the midline crossing frequency per segments in each of the indicated genotypes (n=180, 130, 446, 392, 976 and 488 segments, respectively). Statistically significant differences are denoted by an asterisk (control, *robo*^{2}/+; P<0.001). Scale bar: 10 μm.

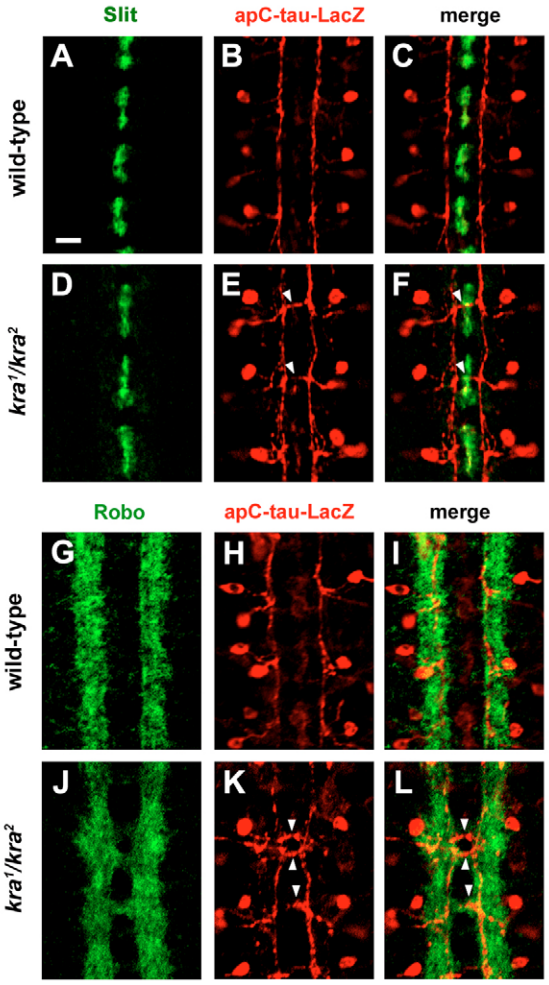

Fig. 6. Robo-positive axons cross the CNS midline in *kra* mutant embryos. (**A-F**) Stage 16 embryos carrying the *apC-tau-lacZ* marker were doubly stained with anti-Slit (A,D) and anti-β-galactosidase (B,E). (A-C) A wild-type embryo. (D-F) A *kra*^{1}/*kra*^{2} mutant embryo; some Ap axons ectopically cross the midline (arrowheads in E,F). (**G-L**) Stage 16 embryos carrying the *apC-tau-lacZ* marker were doubly stained with anti-Robo (G,J) and anti-β-galactosidase (H,K). (G-I) A wild-type embryo. (J-L) A *kra*^{1}/*kra*^{2} mutant embryo; Robo is abnormally detected in the commissural tracts that contain Ap axons crossing the midline (arrowheads in K,L). Scale bar: 10 μm.

The ability of Robo-positive axons to respond to Slit is impaired in *kra* mutant embryos

To further define the role of Kra in midline axon repulsion, we performed detailed phenotypic analyses of *kra* mutant embryos. In the embryonic CNS, glial cells provide neurons with cues and substrata for growth cone migrations (Chotard and Salecker, 2004). Therefore, the axon phenotype observed in *kra* could, in principle, be because of defects in CNS glia. This possibility led us to examine *kra* mutant embryos for glial defects. For this purpose, we also examined the axonal trajectories of the Ap-expressing neurons by introducing an *apC-tau-lacZ* transgene (Lundgren et al., 1995) into the wild-type and *kra* mutant backgrounds. Because Ap axons express Robo (Rajagopalan et al., 2000b), they provide an excellent opportunity to investigate the midline behaviors of Robo-positive axons at single axon resolution. In stage 16 wild-type embryos, the Ap axons remained ipsilateral without crossing the midline (see Fig. S3A,B in the supplementary material) (Lundgren et al., 1995). However, in stage 16 *kra*^{1}/*kra*^{2} embryos, the Ap axons ectopically crossed the midline in 13% of segments despite the apparently normal arrangement of glial cells as defined by anti-Repo and anti-Wrapper (see Fig. S3C,D in the supplementary material). Thus, the ectopic midline crossing of CNS axons in *kra* mutant embryos cannot be ascribed to gross defects in the CNS glia.

We then examined the expression of the midline repellent Slit and its Robo receptor. In stage 16 wild-type embryos, Slit protein was detected at high levels around the midline glia (Fig. 6A,C), whereas Robo was highly expressed on the longitudinal axon tracts

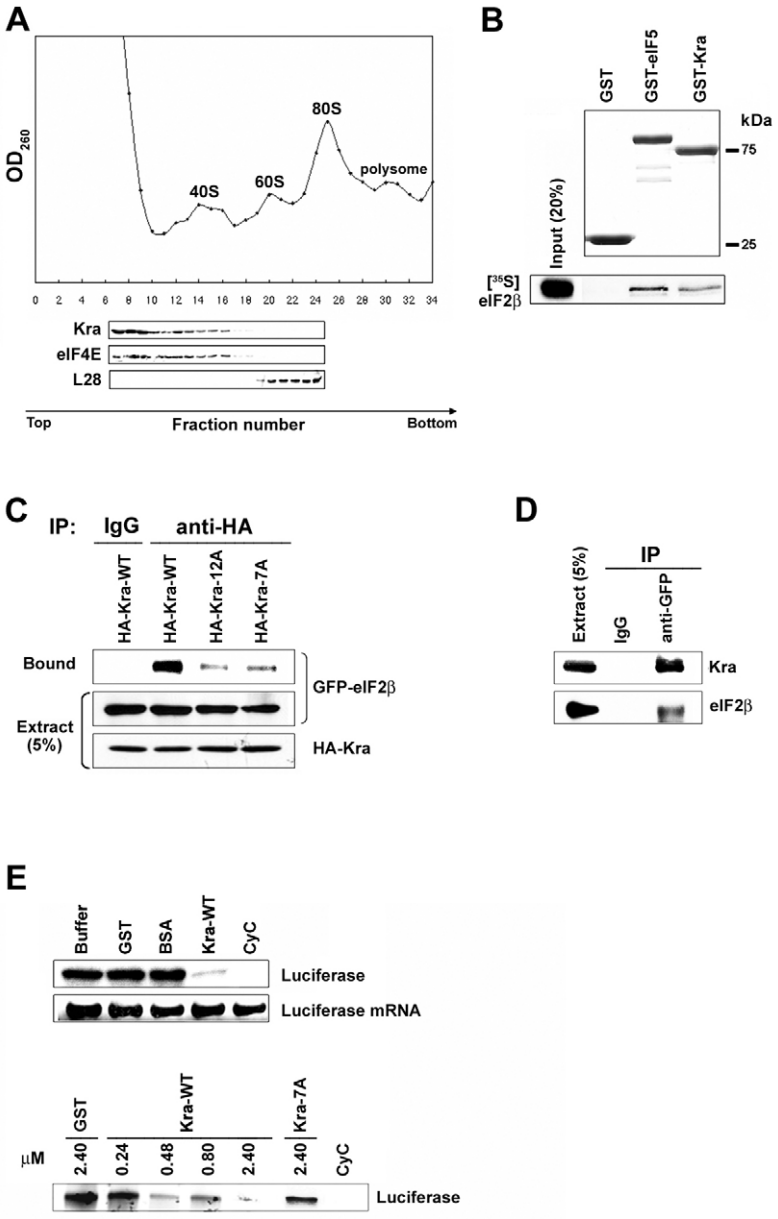

Fig. 7. Kra is a translation inhibitor. (**A**) Kra cosediments with the 40S ribosomal subunit in a sucrose gradient of S2 cell extracts. Cell extracts were prepared in the presence of 100 μg/ml cycloheximide and fractionated on a 7-47% sucrose gradient. Fractions were analyzed for absorbance at 260 nm and subjected to SDS-PAGE and western blot analysis using anti-Kra, anti-eIF4E and anti-L28 antibodies. Positions of 40S and 60S ribosomal subunits, 80S ribosomes, and polysomes are indicated. (**B**) Kra binds eIF2β in vitro. An SDS-gel stained with Coomassie Blue shows GST, GST-eIF5 and GST-Kra proteins in the amounts used for pull-down assays (top panel). A recombinant GST-Kra fusion protein, but not GST alone, interacts with [^{35}S]methionine-labeled eIF2β (bottom panel). GST-eIF5 was used as a positive control for binding. (**C**) The AA-boxes in the W2 domain of Kra are important for its efficient binding to eIF2β in vivo. HA-tagged Kra-WT, -12A, or -7A was coexpressed with GFP-tagged eIF2β in the *Drosophila* embryo. Embryo extracts were immunoprecipitated with anti-HA, and the precipitated eIF2β was detected by western blot analysis using anti-GFP. (**D**) Shot and eIF2β can simultaneously bind to Kra. Soluble extracts of S2 cells overexpressing C-Shot L-GFP were immunoprecipitated with anti-GFP or IgG, and the presence of endogenous Kra and eIF2β in the precipitates was determined by western blot analysis using either anti-Kra or anti-eIF2β antibody, respectively. (**E**) Kra inhibits translation in vitro. In the top panel, *luciferase* mRNA was translated in reticulocyte lysates with [^{35}S]methionine in the absence and presence of the indicated proteins (2.4 μM); reaction samples were analyzed by SDS-PAGE and autoradiography. Translation of *luciferase* mRNA is specifically inhibited by the addition of Kra. In the middle panel, 10% of each reaction was removed after incubation and analyzed by RT-PCR for the presence of *luciferase* mRNA. In the bottom panel, the indicated amounts of GST, Kra-WT and Kra-7A were added to reticulocyte lysates. Cyc, cycloheximide (100 μg/ml).

and largely absent from the commissural tracts (Fig. 6G,I) (Kidd et al., 1999). In the same embryos, the Ap axons remained ipsilateral within the Robo-positive longitudinal tracts (Fig. 6B,C,H,I). However, in stage 16 kra^1/kra^2 embryos, the Ap axons ectopically crossed the midline despite normal Slit expression along the midline (Fig. 6D-F). Surprisingly, Robo protein was aberrantly detected in some commissural axon tracts (Fig. 6J). The commissural tracts expressing Robo frequently contained Ap axons that were ectopically crossing the midline (Fig. 6K,L), suggesting that these axons contribute to aberrant Robo expression. By contrast, Robo expression in the longitudinal axon tracts of *kra* mutant embryos was approximately the same as that of wild-type embryos (Fig. 6G,J). Taken together, these data support an essential role of Kra in maintaining the sensitivity of Robo-expressing growth cones to the midline repellent Slit. However, we cannot exclude the possibility that Robo misexpression by axons normally crossing the midline also contributes to aberrant Robo expression in *kra* mutant embryos.

Kra binds to translation initiation factors and inhibits translation in vitro

All other proteins containing the W2 domain are translation initiation factors and associate with 40S ribosomal subunits (Preiss and Hentze, 2003). To determine whether Kra also associates with 40S ribosomal subunits, *Drosophila* S2 cells were treated with cycloheximide to arrest translation, and their extracts were fractionated on sucrose gradients. Kra cosedimented with the mRNA cap-binding protein eIF4E, but not with the ribosomal protein L28, suggesting that it is associated with 40S, but not 60S, subunits (Fig. 7A).

The W2 domains of eIF5 and eIF2Bε bind directly to the initiation factor eIF2β (Asano et al., 1999), the β-subunit of eIF2 whose GTPase activity is essential for 40S and 60S subunits joining into 80S complexes. eIF5 is a GTPase activating protein (GAP), and eIF2Bε is a GDP exchange factor (GEF) for eIF2. We therefore asked whether Kra also binds to eIF2β through its W2 domain. We found that GST-Kra binds to eIF2β in vitro (Fig. 7B). We observed

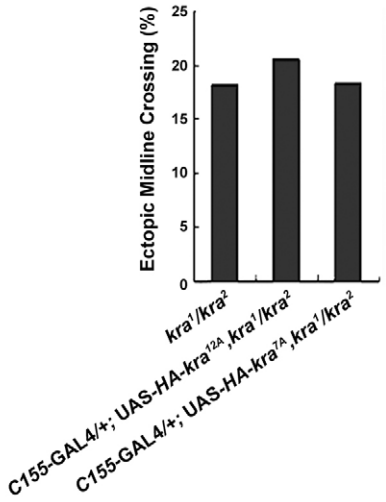

Fig. 8. The Kra AA-boxes 1 and 2 are essential for Kra functionality in vivo. When expressed under the control of the panneuronal driver *C155-GAL4*, neither *UAS-HA-kra^{12A}* nor *UAS-HA-kra^{7A}* rescues the *kra^{1}/kra^{2}* mutant phenotype at the midline (n=312 and 360, respectively). Note that *UAS-HA-kra^{WT}* significantly attenuates the midline crossing phenotype (see Fig. 4F,L).

this interaction in the fly embryo as well (Fig. 7C). Both 12A and 7A mutations significantly impaired Kra binding to eIF2β (Fig. 7C), suggesting that the binding of Kra to eIF2β requires the residues in its W2 domain previously identified as necessary for eIF5 binding to eIF2β (Asano et al., 1999). Because the same W2 domain also binds to Shot, we tested whether the formation of a multiprotein complex containing Shot, Kra and eIF2β is possible. In S2 cells, C-Shot L-GFP coimmunoprecipitated with endogenous Kra and eIF2β (Fig. 7D). As C-Shot L does not directly bind to eIF2β (data not shown), this result suggests that Kra can simultaneously bind to Shot and eIF2β in vivo.

Our results described above suggested that Kra may compete with eIF5 and eIF2Bε for eIF2β. We therefore tested whether Kra inhibits translation in vitro. Translation of *luciferase* mRNA in reticulocyte lysate was specifically inhibited by Kra, but not by BSA and GST control proteins (Fig. 7E). Importantly, we found that these proteins do not affect the stability of *luciferase* mRNA (Fig. 7E). Translation inhibition by Kra was dose-dependent at concentrations ranging from 240 nM to 2.4 μM (Fig. 7E). Interestingly, the 7A mutation significantly impairs Kra activity to inhibit translation (Fig. 7E), suggesting that protein-protein interactions through the AA-box 2 of Kra may be essential for its activity to inhibit translation. The extreme insolubility of Kra-12A in *E. coli* or insect cells prevented us from including it in this assay.

Protein-protein interactions through the W2 domain of Kra are essential for midline axon repulsion

Our biochemical data suggested that the AA-boxes in the W2 domain of Kra are crucial for the formation of complexes containing Shot and eIF2β. To directly test the importance of these protein-protein interaction domains in axon guidance, we tested whether mutations in the AA-boxes would impair the ability of Kra to rescue *kra* mutant phenotypes in the embryonic CNS. Neuronal expression of Kra12A or Kra-7A failed to rescue the midline guidance defect in *kra^{1}/kra^{2}* embryos (Fig. 8). The expression levels and solubility of Kra-12A and Kra-7A were comparable to those observed for the wild-type Kra (data not shown). Thus, the ability of Kra to form protein complexes with Shot and eIF2β is essential for its function in midline axon repulsion.

To confirm the implication of the Kra binding partner eIF2β in midline axon repulsion, we looked at CNS axons in *eIF2β* mutant embryos. We observed ectopic midline crossing by the Ap axons and axons from the pCC ipsilateral pathway (see Fig. S4 in the supplementary material), which is reminiscent of the *kra* loss-of-function phenotypes. This observation further supports a role for eIF2β in Kra-mediated midline axon repulsion and provides in vivo evidence for the requirement of protein translation in axon guidance.

DISCUSSION

kra encodes a novel translation inhibitor required for midline axon guidance

Kra and its human homolog BZAP45 contain an N-terminal leucine-zipper domain of unknown function and a C-terminal W2 domain. We show here that Kra can bind to eIF2β through its W2 domain and inhibit translation in vitro. It is very likely that Kra competes with eIF5 and eIF2Bε for the common binding partner eIF2β, thus inhibiting the assembly of functional preinitiation complexes. A similar mode of translation inhibition has been proposed for DAP-5/p97, which may compete with its homolog eIF4G for eIF3 and eIF4A, thus reducing both cap-dependent and -independent translation (Imataka et al., 1997; Yamanaka et al., 1997). However, the step in translation initiation that is regulated by Kra remains to be addressed experimentally.

Kra-mediated translational repression appears to be an important mechanism underlying midline axon guidance. In the *kra* mutant embryos, Fas II-positive CNS axons that normally remain ipsilateral cross the midline ectopically. This phenotype is observed with the pCC axons from early stages (stages 12 and 13) of axogenesis when they pioneer one of the Fas II pathways. The introduction of multiple alanine substitutions (12A and 7A) into Kra significantly reduces its ability to bind eIF2β and abolishes its activity to rescue the *kra* mutant phenotype, suggesting that the function of Kra in axon guidance depends on its interaction with eIF2β. Consistent with this conclusion, mutations in the *eIF2β* gene also lead to the ectopic midline crossing of Fas II-positive axons.

Shot couples cytoskeleton reorganization to translational control during neuronal morphogenesis

There is a growing body of evidence that F-actin and microtubules are coordinately assembled to each other during axon extension and guidance (Kalil and Dent, 2005; Schaefer et al., 2002; Zhou et al., 2002). Interactions of filopodial actin bundles and microtubules are key features of filopodial maturation into an axon (Sabry et al., 1991) and of growth cone turning (Zhou et al., 2002). Shot, a conserved molecule that scaffolds F-actin, microtubules and the microtubule plus end-binding protein EB1 (Lee and Kolodziej, 2002b; Subramanian et al., 2003), is a strong candidate to bring microtubule plus ends into contact with F-actin bundles. Indeed, Shot is required for the extension of sensory and motor axons (Lee and Kolodziej, 2002b), and a mammalian homolog of Shot, ACF7, is required for microtubules to track along F-actin cables towards the leading edge of spreading endodermal cells (Kodama et al., 2003). Thus, previous studies have suggested that Shot/ACF7 coordinately organizes F-actin and microtubules to support the motility of neuronal growth cones and nonneuronal cells.

Our findings suggest that Shot also functions together with the translation inhibitor Kra to control midline axon repulsion. Shot physically associates with Kra in vivo. The *shot* loss-of-function phenotype at the CNS midline is reminiscent of the *kra* loss-of-function phenotype. The major Kra-binding domain in Shot is required for its role in midline axon repulsion. Moreover, *shot* and *kra* genetically interact in a dosage-sensitive manner for the midline phenotype. Our data also support the idea that cytoskeletal assembly and translational regulation can occur in a coordinated way. We found that midline axon repulsion requires both the activity of Kra to recruit eIF2β and the activity of Shot to bind to F-actin. Thus, it is likely that local levels of eIF2β available for protein synthesis can be spatially regulated with regard to actin cytoskeleton remodeling during axon guidance.

Shot/Kra mode of action in midline axon repulsion

In *Drosophila*, Slit is the key ligand driving midline axon repulsion (Kidd et al., 1999), and therefore midline crossing of CNS growth cones is primarily controlled by the Robo receptor of Slit (Rajagopalan et al., 2000a). How then do neurons regulate levels of Robo on the surface of their axons and growth cones? The transmembrane protein Commissureless (Comm) has been shown to dynamically regulate Robo expression (Keleman et al., 2002; Myat et al., 2002). Comm functions as an intracellular sorting receptor to target newly made Robo for lysosomal degradation, thereby blocking its transport to the growth cone that is crossing the midline (Keleman et al., 2002; Keleman et al., 2005).

Translational regulation has also been shown to alter the responsiveness of growth cones to the midline repellents (Dickson, 2002). In vitro studies of cultured embryonic retinal ganglion cells (RGCs) provided an insight into how translation is regulated in axons and growth cones in response to midline guidance cues. Treatment of these neurons with netrin-1 leads to the rapid activation of signaling pathways that phosphorylate the translation initiation factor eIF4E and its binding protein eIF4E-BP1 and thus induces axonal protein synthesis (Campbell and Holt, 2001; Campbell and Holt, 2003). Our data presented here indicate that the role of Kra in midline axon repulsion depends on its ability to recruit the translation initiation factor eIF2β to Shot. Thus, protein complexes containing Shot, Kra and eIF2β may function as additional targets for signaling systems that critically control axon guidance at the CNS midline. Regulation of Shot-Kra-eIF2β complexes may occur in neuronal cell bodies, where Kra is concentrated, or in axons and growth cones, which may require local protein synthesis to meet developmental requirements. In the latter case, as Kra is not detectable in the CNS axons of the *Drosophila* embryo, even a low amount of Kra may be sufficient for guiding axons.

Intriguingly, Robo was aberrantly detected on commissural axons in kra^{1}/kra^{2} mutant embryos. Given the increased frequency of ectopic crossovers in these embryos, as well as the documented role of Robo in preventing axons from crossing the midline (Kidd et al., 1998), this finding is somewhat paradoxical. One possibility is that Kra, induced by interaction with Shot and eIF2β, could repress the synthesis of as yet unidentified proteins that transduce or modulate Robo signaling. In *shot* or *kra* mutant embryos, perhaps this translational regulatory circuit is not activated, and thus Robo-expressing growth cones abnormally cross the midline because of a decrease in the strength of Robo signaling output. Alternatively, Kra may function to finely tune the expression levels of their multiple targets that mediate attractive or repulsive responses. In this scenario, impairment of the Shot-Kra-eIF2β circuit could disturb the precise balance between repulsion and attraction signaling at the midline, thereby decreasing the overall sensitivity of Robo-expressing growth cones to Slit. Therefore, efforts to reveal the direct targets of Kra-mediated repression in the future may provide better insights into the immediate mechanisms by which translational regulation plays an essential role for midline axon repulsion.

We thank Haejung Won for her able technical assistance, and Changjoon Justin Lee, Kei Cho and Andy Furley for their valuable comments. We thank Akira Nakamura for the anti-eIF4E antibody, Edward Giniger for the *apC-tau-lacZ* transgenic line, Sang-Hak Jeon for the *repo-GAL4* line and Christian Klämbt for the *slit-GAL4* line. This work was supported by funds from the Brain Research Center of the 21st Century Frontier, the Basic Research Program of the Korea Science and Engineering Foundation (R01-2006-000-10487-0) and the Korea Research Foundation (KRF-2003-015-C00472 and KRF-2006-0409-20060081).

Supplementary material

Supplementary material for this article is available at http://dev.biologists.org/cgi/content/full/134/9/1767/DC1

References

Asano, K., Krishnamoorthy, T., Phan, L., Pavitt, G. D. and Hinnebusch, A. G. (1999). Conserved bipartite motifs in yeast eIF5 and eIF2Bepsilon, GTPase-activating and GDP-GTP exchange factors in translation initiation, mediate binding to their common substrate eIF2. *EMBO J.* **18**, 1673-1688.

Brand, A. H. and Perrimon, N. (1993). Targeted gene expression as a means of altering cell fates and generating dominant phenotypes. *Development* **118**, 401-415.

Brittis, P. A., Lu, Q. and Flanagan, J. G. (2002). Axonal protein synthesis provides a mechanism for localized regulation at an intermediate target. *Cell* **110**, 223-235.

Campbell, D. S. and Holt, C. E. (2001). Chemotropic responses of retinal growth cones mediated by rapid local protein synthesis and degradation. *Neuron* **32**, 1013-1026.

Campbell, D. S. and Holt, C. E. (2003). Apoptotic pathway and MAPKs differentially regulate chemotropic responses of retinal growth cones. *Neuron* **37**, 939-952.

Chotard, C. and Salecker, I. (2004). Neurons and glia: team players in axon guidance. *Trends Neurosci.* **27**, 655-661.

Chou, T. B., Noll, E. and Perrimon, N. (1993). Autosomal P[ovoD1] dominant female-sterile insertions in *Drosophila* and their use in generating germ-line chimeras. *Development* **119**, 1359-1369.

Clemens, J. C., Worby, C. A., Simonson-Leff, N., Muda, M., Maehama, T., Hemmings, B. A. and Dixon, J. E. (2000). Use of double-stranded RNA interference in Drosophila cell lines to dissect signal transduction pathways. *Proc. Natl. Acad. Sci. USA* **97**, 6499-6503.

Dent, E. W. and Gertler, F. B. (2003). Cytoskeletal dynamics and transport in growth cone motility and axon guidance. *Neuron* **40**, 209-227.

Dickson, B. J. (2002). Molecular mechanisms of axon guidance. *Science* **298**, 1959-1964.

Dubnau, J., Chiang, A. S., Grady, L., Barditch, J., Gossweiler, S., McNeil, J., Smith, P., Buldoc, F., Scott, R., Certa, U. et al. (2003). The staufen/pumilio pathway is involved in Drosophila long-term memory. *Curr. Biol.* **13**, 286-296.

Halter, D. A., Urban, J., Rickert, C., Ner, S. S., Ito, K., Travers, A. A. and Technau, G. M. (1995). The homeobox gene repo is required for the differentiation and maintenance of glia function in the embryonic nervous system of Drosophila melanogaster. *Development* **121**, 317-332.

Imataka, H., Olsen, H. S. and Sonenberg, N. (1997). A new translational regulator with homology to eukaryotic translation initiation factor 4G. *EMBO J.* **16**, 817-825.

Kalil, K. and Dent, E. W. (2005). Touch and go: guidance cues signal to the growth cone cytoskeleton. *Curr. Opin. Neurobiol.* **2**, 521-526.

Keleman, K., Rajagopalan, S., Cleppien, D., Teis, D., Paiha, K., Huber, L. A., Technau, G. M. and Dickson, B. J. (2002). Comm sorts robo to control axon guidance at the Drosophila midline. *Cell* **110**, 415-427.

Keleman, K., Ribeiro, C. and Dickson, B. J. (2005). Comm function in commissural axon guidance: cell-autonomous sorting of Robo in vivo. *Nat. Neurosci.* **8**, 156-163.

Kidd, T., Brose, K., Mitchell, K. J., Fetter, R. D., Tessier-Lavigne, M., Goodman, C. S. and Tear, G. (1998). Roundabout controls axon crossing of the CNS midline and defines a novel subfamily of evolutionarily conserved guidance receptors. *Cell* **92**, 205-215.

Kidd, T., Bland, K. S. and Goodman, C. S. (1999). Slit is the midline repellent for the robo receptor in Drosophila. *Cell* **96**, 785-794.

Kodama, A., Karakesisoglou, I., Wong, E., Vaezi, A. and Fuchs, E. (2003). ACF7: an essential integrator of microtubule dynamics. *Cell* **115**, 343-354.

Lee, S. and Kolodziej, P. A. (2002a). The plakin Short Stop and the RhoA GTPase

are required for E-cadherin-dependent apical surface remodeling during tracheal tube fusion. *Development* **129**, 1509-1520.
Lee, S. and Kolodziej, P. A. (2002b). Short Stop provides an essential link between F-actin and microtubules during axon extension. *Development* **129**, 1195-1204.
Lee, S., Harris, K. L., Whitington, P. M. and Kolodziej, P. A. (2000). short stop is allelic to kakapo, and encodes rod-like cytoskeletal-associated proteins required for axon extension. *J. Neurosci.* **20**, 1096-1108.
Lin, D. M. and Goodman, C. S. (1994). Ectopic and increased expression of Fasciclin II alters motoneuron growth cone guidance. *Neuron* **13**, 507-523.
Lundgren, S. E., Callahan, C. A., Thor, S. and Thomas, J. B. (1995). Control of neuronal pathway selection by the Drosophila LIM homeodomain gene apterous. *Development* **121**, 1769-1773.
Ming, G. L., Wong, S. T., Henley, J., Yuan, X. B., Song, H. J., Spitzer, N. C. and Poo, M. M. (2002). Adaptation in the chemotactic guidance of nerve growth cones. *Nature* **417**, 411-418.
Myat, A., Henry, P., McCabe, V., Flintoft, L., Rotin, D. and Tear, G. (2002). Drosophila Nedd4, a ubiquitin ligase, is recruited by Commissureless to control cell surface levels of the roundabout receptor. *Neuron* **35**, 447-459.
Nakamura, A., Sato, K. and Hanyu-Nakamura, K. (2004). Drosophila cup is an eIF4E binding protein that associates with Bruno and regulates oskar mRNA translation in oogenesis. *Dev. Cell* **6**, 69-78.
Noordermeer, J. N., Kopczynski, C. C., Fetter, R. D., Bland, K. S., Chen, W. Y. and Goodman, C. S. (1998). Wrapper, a novel member of the Ig superfamily, is expressed by midline glia and is required for them to ensheath commissural axons in Drosophila. *Neuron* **21**, 991-1001.
O'Keefe, D. D., Thor, S. and Thomas, J. B. (1998). Function and specificity of LIM domains in *Drosophila* nervous system and wing development. *Development* **125**, 3915-3923.
Preiss, T. and Hentze, M. W. (2003). Starting the protein synthesis machine: eukaryotic translation initiation. *BioEssays* **25**, 1201-1211.
Rajagopalan, S., Nicolas, E., Vivancos, V., Berger, J. and Dickson, B. J. (2000a). Crossing the midline: roles and regulation of Robo receptors. *Neuron* **28**, 767-777.
Rajagopalan, S., Vivancos, V., Nicolas, E. and Dickson, B. J. (2000b). Selecting a longitudinal pathway: Robo receptors specify the lateral position of axons in the Drosophila CNS. *Cell* **103**, 1033-1045.
Robertson, H. M., Preston, C. R., Phillis, R. W., Johnson-Schlitz, D. M., Benz, W. K. and Engels, W. R. (1988). A stable genomic source of P element transposase in Drosophila melanogaster. *Genetics* **118**, 461-470.
Sabry, J. H., O'Connor, T. P., Evans, L., Toroian-Raymond, A., Kirschner, M. and Bentley, D. (1991). Microtubule behavior during guidance of pioneer neuron growth cones in situ. *J. Cell Biol.* **115**, 381-395.
Schaefer, A. W., Kabir, N. and Forscher, P. (2002). Filopodia and actin arcs guide the assembly and transport of two populations of microtubules with unique dynamic parameters in neuronal growth cones. *J. Cell Biol.* **158**, 139-152.
Scholz, H., Sadlowski, E., Klaes, A. and Klambt, C. (1997). Control of midline glia development in the embryonic Drosophila CNS. *Mech. Dev.* **64**, 137-151.
Sepp, K. J., Schulte, J. and Auld, V. J. (2001). Peripheral glia direct axon guidance across the CNS/PNS transition zone. *Dev. Biol.* **238**, 47-63.
Simpson, J. H., Bland, K. S., Fetter, R. D. and Goodman, C. S. (2000). Short-range and long-range guidance by Slit and its Robo receptors: a combinatorial code of Robo receptors controls lateral position. *Cell* **103**, 1019-1032.
Song, H. and Poo, M. (2001). The cell biology of neuronal navigation. *Nat. Cell Biol.* **3**, E81-E88.
Spencer, S. A., Powell, P. A., Miller, D. T. and Cagan, R. L. (1998). Regulation of EGF receptor signaling establishes pattern across the developing Drosophila retina. *Development* **125**, 4777-4790.
Subramanian, A., Prokop, A., Yamamoto, M., Sugimura, K., Uemura, T., Betschinger, J., Knoblich, J. A. and Volk, T. (2003). Shortstop recruits EB1/APC1 and promotes microtubule assembly at the muscle-tendon junction. *Curr. Biol.* **13**, 1086-1095.
Wodarz, A., Hinz, U., Engelbert, M. and Knust, E. (1995). Expression of crumbs confers apical character on plasma membrane domains of ectodermal epithelia of Drosophila. *Cell* **82**, 67-76.
Yamanaka, S., Poksay, K. S., Arnold, K. S. and Innerarity, T. L. (1997). A novel translational repressor mRNA is edited extensively in livers containing tumors caused by the transgene expression of the apoB mRNA-editing enzyme. *Genes Dev.* **11**, 321-333.
Zhou, F. Q., Waterman-Storer, C. M. and Cohan, C. S. (2002). Focal loss of actin bundles causes microtubule redistribution and growth cone turning. *J. Cell Biol.* **157**, 839-849.